Pramāṇa, Vol. 5, No. 4, 1975, pp. 211–226. © Printed in India.

Cosmic ray muons at a depth of 754 hg/cm² in the Kolar Gold Mines

M R KRISHNASWAMY, M G K MENON and V S NARASIMHAM
Tata Institute of Fundamental Research, Bombay 400005

N ITO, S KAWAKAMI and S MIYAKE*
Osaka City University, Osaka, Japan

MS received 21 July 1975; in revised form 16 August 1975

Abstract. A telescope of area 4 m², consisting of horizontal layers of plastic scintillators, neon flash tubes and absorbers was operated at a depth of 754 hg/cm² in the Kolar Gold Mines. New values for the vertical intensities of muons have been obtained from observations of the angular distribution over the slant depths ~ 750–2300 hg/cm² and are compared with the existing measurements. From the angular distribution observed, we conclude that muons are produced wholly through the decay of pions and kaons up to energies of the order of 1 TeV. A value of $0{\cdot}3 \pm 0{\cdot}2$ is estimated for the K/π ratio at production, for muon energies around 500 GeV. A decoherence distribution has been obtained for parallel muon events up to distances of the order of 10 m. From this we conclude that the average P_t of the parents of muons of energy ~ 250 GeV is of the order of 0·3 GeV/c. From an analysis of rock showers, we obtain the cross section for inelastic interaction of muons of mean energy 100 GeV as $(3{\cdot}8 \pm 1{\cdot}5) \times 10^{-30}$ cm²/nucleon.

Keywords. Cosmic ray muons; underground experiments; angular distribution; inelastic cross section of muons.

1. Introduction

In the past, deep underground cosmic ray muon experiments have been conducted at a variety of depths under widely different rock formations. In the early experiments, simple telescopes consisting of GM counters and scintillators using coincidence methods were employed for the determination of vertical muon intensities and angular distributions. More recently, sophisticated arrays of larger area incorporating visual detectors have been operated underground. The present series of experiments in the Kolar Gold Mines in South India are designed to measure the angular distribution of muons with good statistical precision, over a wide range of angles, and at a variety of depths underground chosen in such a manner that meaningful inter-comparison of data can be made up to very great depths. So far, measurements have been completed at three depths of 816 ft, 1612 ft and 3655 ft; measurements are now in progress at a depth of 6525 ft. A brief presentation of the observations at 816 ft was made earlier by Krishna-

* Now at the Cosmic Ray Laboratory, University of Tokyo, Tokyo, Japan.

swamy *et al* (1969). In this paper, a detailed report of the work at the depth of 816 ft is presented.

2. Experimental details

2·1. *Muon detector*

A schematic diagram of the detector is shown in figure 1. The detector comprised of a horizontal layer of area 4 m^2 of plastic scintillators of thickness 5 cm. This was arranged in 4 equal areas (B_1, B_2, B_3 and B_4) each of 1 m^2 to complete a square of 2 m × 2 m. Each 1 m^2 area was viewed by 3 photomultipliers of the type Dumont 6364. Below the scintillator layer, there were 4 slabs of visual detector, comprising of neon flash tube (NFT) trays. A tray comprised of 4 horizontal layers of staggered NFT's, 2 m in length and 2 cm in diameter; the alternate slabs were arranged in an orthogonal geometry, to enable measurement of the spacial angles of the tracks. With this array, the zenith angle, θ, could be measured to an accuracy better than $\pm 1{\cdot}5°$; the accuracy improves with increasing zenith angle since the particle traverses a longer distance striking many NFT's; typically, the error is $\pm 0{\cdot}5°$ at $\theta = 60°$.

On top of each NFT tray, there was a layer of $\frac{1}{2}''$ thick lead resting on $\frac{1}{4}''$ thick iron plate. The minimum energy required to penetrate the detector in the vertical direction is ~ 150 MeV. At any other zenith angle the minimum energy required is $\sim 150 \times \sec\theta$ MeV.

2·2. *Triggering*

A 3-fold coincidence within a resolving time of about one microsecond, between pulses from the photomultipliers viewing any 1 m^2 area of scintillator, provided the trigger for applying the high voltage pulse to the NFT array. The flashes from the crossed NFT's were photographed by a camera through a suitable mirror system.

The triggering rate was about 170 per hour for each 1 m^2 area. Out of this, the rate of muons is 118 per hour and the rest is due to gamma-rays from radioactive substances in the surrounding rock. Since the background radiation is of very low energy ($\leqslant 2$ MeV), the secondary electrons are stopped by the scintillator itself, and hence there is no ambiguity in the measurement of the rate of muons traversing the detector; the latter is actually obtained from the photographs of tracks in the NFT array. Since the rate of collection of muons is very high, only 1 m^2 area of the plastic scintillator was used for triggering at any time during the period of operation of the detector. In view of the exact symmetry of the 4 scintillation detectors, the rate of in-geometry muons passing through the entire detector is exactly 4 times that recorded with 1 m^2 area.

The telescope was operated for a total period of $1{\cdot}12 \times 10^6$ seconds; the 4 scintillator areas, B_1, B_2, B_3 and B_4, were used for triggering for $1{\cdot}83 \times 10^5$, $2{\cdot}23 \times 10^5$, $5{\cdot}35 \times 10^5$ and $1{\cdot}8 \times 10^5$ seconds respectively. The overall live time of observation, after allowing for the dead-time of the electronics, is obtained as $8{\cdot}55 \times 10^5$ seconds, and during this period $2{\cdot}74 \times 10^4$ events have been recorded.

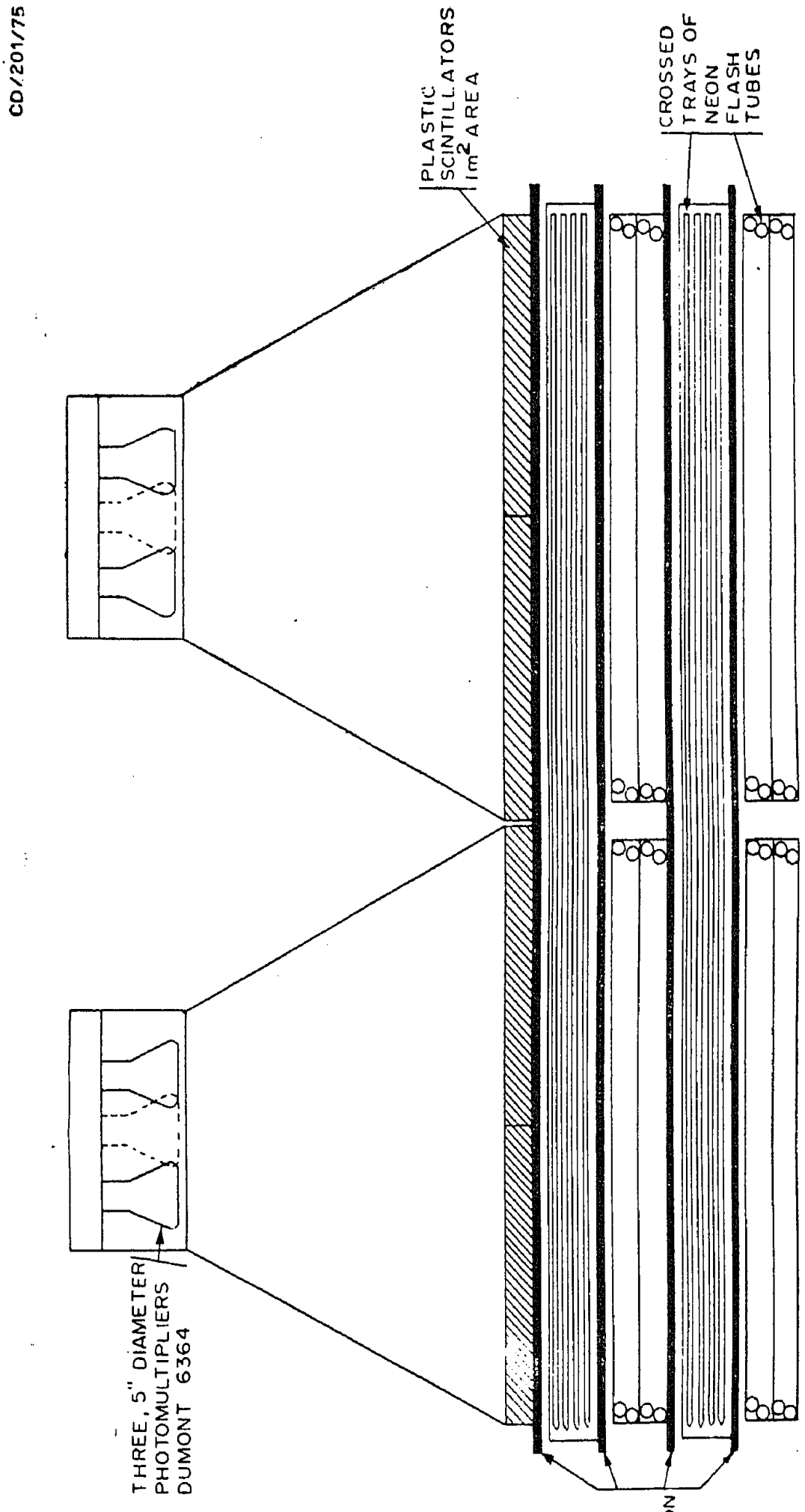

Figure 1. A schematic diagram of the vertical telescope at the depth of 754 hg/cm² in the Kolar Gold Mines.

2.3. *Details of surface topography and the density of rock*

The detector was located at the 8th level of the New Trial Shaft at a distance of ~ 50 meters from the rim of the shaft. The vertical depth from the collar of the shaft to the level of observation is 816 feet. The topography of the Kolar Gold Fields around the New Trial Shaft is reasonably uniform within a circle of radius ~ 750 meters (which corresponds to an angular range of 0°–75° at the 8th level) with a maximum deviation of $\pm$ 15 m from the average level. Actually, the region covered by B_3 trigger is flatter than other parts of the surface. Hence B_3 trigger was employed for a large fraction of the period of observation.

The average density of rock is found to be 3·03 g/cm^3 from measurements made on 12 samples collected from various depths above the 8th level of New Trial Shaft. This value is in good agreement with the earlier ones (Krishnaswamy *et al* 1968, Miyake *et al* 1964) which were based on rock samples collected from a different part of the mining complex. The maximum possible uncertainty on the density of rock is 1%. The vertical depth of the present observation is estimated as 754 hg/cm^2 (Kolar) below ground level.

3. Angular distribution and vertical intensity of muons

3.1. *Basic data*

Since the total number of muons recorded is very large, only a third of the data has been considered for the angular distribution for $\theta < 50°$; whereas most of the available data have been used for $\theta \geqslant 50°$.

In table 1, we present all the relevant details concerning the experimental data; the angular intervals, number of events per interval and the observed rates of events per sec in each angular bin are given in columns 1, 3 and 4 of this table respectively. The errors shown for the observed rate of events are wholly statistical in nature.

3.2. *Slant depths*

To make accurate estimates of the rate of events in each angular interval and then to obtain a reliable depth-intensity relation from the present measurements, it is necessary to determine the slant depths corresponding to the entire range of angular intervals between 0–75°. The surface topography around the New Trial Shaft is available in the form of contour maps showing elevation or depression with reference to a datum level in 5 ft intervals. From these maps, we can determine the average values of surface levels (*i.e.*, the vertical height, h_s, above the level of observation) for 5° × 10° bins in zenithal and azimuthal angles. A weighted average of surface levels is taken over the azimuthal bins to obtain a mean value for each zenithal bin of 5°. The effective slant depths are then calculated for each angle, θ, as $h_s \times \sec \theta$. We show, in column 2 of table 1, the effective slant depths below ground level for the mean zenith angle θ_m, of each bin of 5°.

3.3. *Expected rate of muons*

The rate of muons for a 5° interval of zenith angle can be expressed as;

Table

Angular Range (Degrees)	Effective Slant Depth (hg/cm²)	Number of Events	Observed Rate* (No./sec)	Expected Rate (No./sec)	Vertical Intensity+ (Muons/cm². sec. sterad)
0–5	753	358	$(7{\cdot}97 \pm 0{\cdot}42) \times 10^{-4}$	$7{\cdot}04 \times 10^{-4}$	$(2{\cdot}78 \pm 0{\cdot}07) \times 10^{-6}$
5–10	759	882	$(1{\cdot}95 \pm 0{\cdot}07) \times 10^{-3}$	$2{\cdot}1 \times 10^{-3}$	
10–15	770	1224	$(2{\cdot}65 \pm 0{\cdot}08) \times 10^{-3}$	$3{\cdot}22 \times 10^{-3}$	$(2{\cdot}47 \pm 0{\cdot}07) \times 10^{-6}$
15–20	788	1594	$(3{\cdot}42 \pm 0{\cdot}09) \times 10^{-3}$	$4{\cdot}02 \times 10^{-3}$	$(2{\cdot}36 \pm 0{\cdot}06) \times 10^{-6}$
20–25	812	1764	$(3{\cdot}78 \pm 0{\cdot}09) \times 10^{-3}$	$4{\cdot}48 \times 10^{-3}$	$(2{\cdot}25 \pm 0{\cdot}06) \times 10^{-6}$
25–30	844	1873	$(3{\cdot}98 \pm 0{\cdot}09) \times 10^{-3}$	$4{\cdot}57 \times 10^{-3}$	$(2{\cdot}00 \pm 0{\cdot}06) \times 10^{-6}$
30–35	890	1789	$(3{\cdot}76 \pm 0{\cdot}09) \times 10^{-3}$	$4{\cdot}40 \times 10^{-3}$	$(1{\cdot}73 \pm 0{\cdot}05) \times 10^{-6}$
35–40	943	1683	$(3{\cdot}50 \pm 0{\cdot}09) \times 10^{-3}$	$3{\cdot}86 \times 10^{-3}$	$(1{\cdot}50 \pm 0{\cdot}04) \times 10^{-6}$
40–45	1014	1418	$(2{\cdot}92 \pm 0{\cdot}08) \times 10^{-3}$	$3{\cdot}18 \times 10^{-3}$	$(1{\cdot}24 \pm 0{\cdot}03) \times 10^{-6}$
45–50	1101	1159	$(2{\cdot}39 \pm 0{\cdot}07) \times 10^{-3}$	$2{\cdot}38 \times 10^{-3}$	$(9{\cdot}99 \pm 0{\cdot}29) \times 10^{-7}$
50–55	1217	1053	$(1{\cdot}57 \pm 0{\cdot}05) \times 10^{-3}$	$1{\cdot}68 \times 10^{-3}$	$(6{\cdot}73 \pm 0{\cdot}21) \times 10^{-7}$
55–60	1370	712	$(1{\cdot}06 \pm 0{\cdot}04) \times 10^{-3}$	$1{\cdot}03 \times 10^{-3}$	$(5{\cdot}00 \pm 0{\cdot}19) \times 10^{-7}$
60–65	1586	341	$(5{\cdot}09 \pm 0{\cdot}28) \times 10^{-4}$	$5{\cdot}02 \times 10^{-4}$	$(2{\cdot}86 \pm 0{\cdot}15) \times 10^{-7}$
65–70	1852	148	$(2{\cdot}21 \pm 0{\cdot}18) \times 10^{-4}$	$2{\cdot}01 \times 10^{-4}$	$(1{\cdot}70 \pm 0{\cdot}14) \times 10^{-7}$
70–75	2277	28	$(4{\cdot}18 \pm 0{\cdot}79) \times 10^{-5}$	$4{\cdot}25 \times 10^{-5}$	$(7{\cdot}50 \pm 1{\cdot}40) \times 10^{-8}$

* Corrected for gaps in NFT array.

+ Errors shown in this column are purely statistical; the vertical intensity inferred from 0–5° and 5°–10° is combined to correspond to a depth of 756 hg/cm².

$$\text{Rate} = \int_{\theta-2{\cdot}5^\circ}^{\theta+2{\cdot}5^\circ} I_v(h)\, R(h, \theta)\, A(\theta)\, d\theta \tag{1}$$

where $I_v(h)$, $A(\theta)$ and $R(h, \theta)$ are vertical intensity at a depth h, differential aperture at θ° and the enhancement factor respectively.

The empirical formula given by Miyake (1963) has been used for $I_v(h)$ in the range of slant depths covered by the present observations. (This is in good agreement with all the available data, as will be shown in section 4.2 of this paper.) The empirical formula can be expressed as follows:

$$I_v(h) = \frac{A}{h+H}(h+a)^{-\alpha} \exp(-\beta h) \tag{2}$$

where $A = 174$, $H = 400$, $a = 11$, $\alpha = 1{\cdot}53$, $\beta = 8{\cdot}0 \times 10^{-4}$ and h is expressed in units of hg/cm².

The differential aperture of the detector for 1 m² trigger is given by

$$A(\theta)\, d\theta = \tfrac{1}{4}(2\pi a^2 - 8\, ad \tan\theta + 2d^2 \tan^2\theta) \sin\theta \cos\theta\, d\theta \qquad (3)$$

where $a = 200$ cm and $d = 53$ cm. The value of 'd' has been obtained by defining an in-geometry muon as one that crossed the central plane of the scintillator layer and the central electrode of the bottom NFT tray; this criterion has been strictly followed in data reduction. The factor $\frac{1}{4}$ in eq. (3) is due to the 1 m^2 trigger.

The enhancement factor $R(h, \theta) = I(h, \theta)/I(h \sec\theta, 0)$, arises from the fact that the parents of muons, *i.e.*, pions and kaons have an increasing probability of decay with increasing zenith angle in the earth's atmosphere. The values of $R(h, \theta)$ are obtained in the following manner.

The differential energy spectrum of pions and kaons are assumed to have the form

$$F_{K\pi}(E)\, dE = A_{K\pi} E^{-\gamma}\, dE \qquad (4)$$

in the energy region 0·2 – 2 TeV, relevant for the present observations. The K/π ratio at production is assumed to be 0·2, consistent with the ISR (CERN) observations on P-P interactions up to 2 TeV. With these assumptions, the ratio of muon intensities at an angle, θ, and in the vertical direction, $I(>E, \theta)/I(>E, 0)$, are derived by a straightforward procedure (*see* for example Maeda 1964). An additional constraint is to make sure that the resultant muon spectrum at $\theta = 0$ is in good agreement with the presently available data, by suitably selecting the values of A and γ. The enhancement factors, $R(h, \theta)$, in terms of depth, h, and angle, θ, are obtained from these ratios by a suitable transformation from energy of muons to the depth. We ignore in this analysis the fluctuations in the energy loss of muons, since $R(h, \theta)$ is insensitive to them in the low energy region.

The expected rates of events for 5° bins of zenith angle as determined from the preceding analysis are shown in column 5 of table 1. In figure 2, the observed rates of events are shown as a histogram. The solid curve in this figure is a representation of eq. 1 in a differential form, drawn through the central angle of each bin, *i.e.*, the rate of events in each bin is obtained as the product of the rate at the central angle and the bin width. It is clear that there is very good agreement between the observations and the expected rates of muons, except for a small ($\sim 10\%$) discrepancy in the 15°–40° interval of zenith angle.

3.4. *Estimation of errors*

The efficiency for detection of muons by the plastic scintillation detectors is found experimentally to be close to 100% for all zenith angles.

At small zenith angles, the error in angle measurement is $\pm 1{\cdot}5°$ for single muons. However, for muons associated with showers, ($< 5\%$ of the total number of events), the error is more; and this varies from one event to another. This could introduce some uncertainty in the classification of events into bins of 5° width in zenith angle. In the present case, however, this affects only the very small angle region, $\theta < 10°$, where the aperture rises very rapidly. For large angles, $\theta > 40°$, in view of the large number of flashes along the trajectory of the

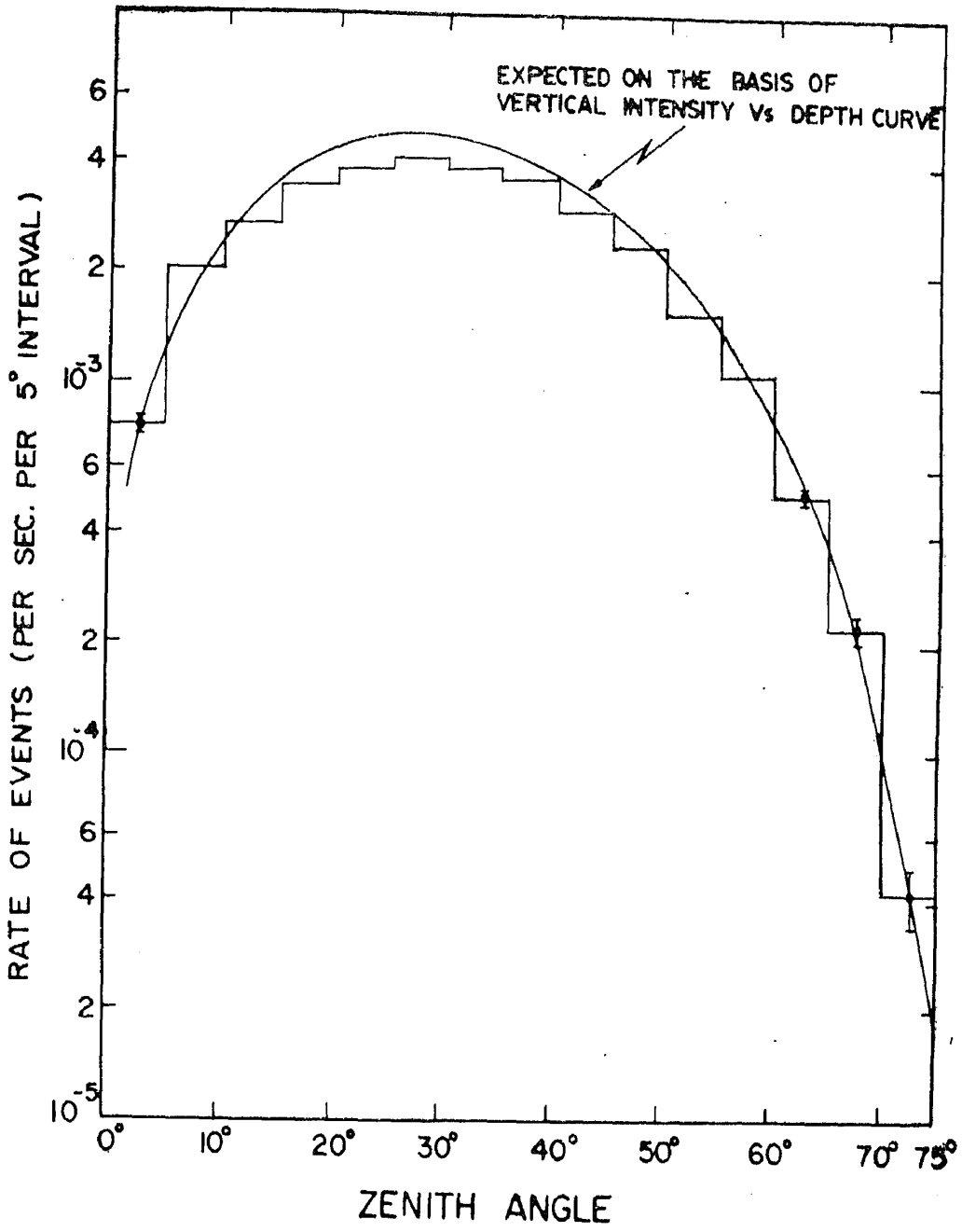

Figure 2. A histogram of the angular distribution of muons at 754 hg/cm². The expected absolute distribution is shown as a smooth curve.

muon, the uncertainty in the angle measurement is very small in almost all types of events.

There are gaps of ~ 8 cm $\times$ 2 m in each horizontal slab of NFT's between the two boxes each of area 1×2 m². A muon passing through the gaps would produce a track in only 2 or 3 of the crossed NFT slabs. For such events, which constitute about a few per cent of the total, the error in the angle is governed by the width of the gaps and the separation between the NFT slabs. These have been analysed separately, in terms of the angular distribution in projected zenith angles, and are found to be in good agreement with estimates based on geometrical factors. The fraction of such events for each bin of 5° ($\sim 8\%$ at 0–5° and gradually decreasing to $\sim 1\%$ at 40°–45°) has been allowed for in determining the rates shown in figure 2 and table.

The differential apertures have been determined analytically for all zenith angles 0–75°. However, due to edge effects arising primarily from the scintillator thickness of 5 cm, there is some uncertainty in the aperture at the very large angular interval 70°–75°; this amounts to $\leqslant 10\%$; and is less than a few per cent at all other angles.

4. Vertical intensity *vs* depth curve

4.1. *Vertical intensity at 754 hg/cm²*

The vertical intensity at the present depth of observation is obtained by dividing the number of muons recorded in a narrow angular interval 0–θ°, near the vertical direction, by the product of the live time of observation and the aperture ($S\Omega$) of the telescope for 0–θ°. The uncertainty in the aperture, due to the angular distribution of muons expressed as $I(h, \theta) = I(h, 0) \cos^n \theta$ with $n \sim 2.0$, is very small as we consider only a small angular region. However, to avoid possible uncertainty due to diffusion of events from one bin to another, we have evaluated the vertical intensity from several angular regions 0–θ_i^0, with θ_i always inside the broad maximum of the histogram in figure 2 and taken an average of these intensities. From this we obtain the vertical intensity at 754 hg/cm² as $(2{\cdot}8 \pm 0{\cdot}1) \times 10^{-6}$ cm^{-2} sec^{-1} sr^{-1}.

4.2. *Vertical intensities inferred from the angular distribution*

The angular distribution of muons, shown in figure 2, is used to derive the vertical intensities at several depths below the level of observation. As shown in section 3.3, the rate of events for each 5° interval of zenith angle can be expressed by eq. 1. In this, $R(h, \theta)$ and the aperture distribution $A(\theta)$ are exactly calculable. It can be shown that the uncertainty in $R(h, \theta)$ due to small variations of the K/π ratio, and the exponent, γ, of the production spectrum (eq. 4), is very small. The aperture distribution, as discussed in section 3.3, is uncertain to $\sim 10\%$ only at the largest angles 70°–75°; but this is still less than the statistical errors. For each bin of zenith angle, we obtain the mean angle, θ_m, from the observed distribution, and an effective slant depth $h \sec \theta_m$. The vertical intensities are derived for these slant depths over the range 754–2277 hg/cm² and are shown in column 6 of table 1 and in figure 3.

The intensities obtained by Achar *et al* (1965), Barton (1961), Barrett *et al* (1952), Bollinger (1951), Castagnoli *et al* (1965), Krishnaswamy *et al* (1969), Miyake *et al* (1964), Sheldon *et al* (1969), Stockel (1969) and Keuffel *et al* (1969) are also shown in this figure for comparison, by suitably correcting them, wherever necessary, to correspond to Kolar rock. The smooth curve drawn in the figure is based on the empirical formula given in eq. 2; this is in reasonable agreement with the intensities derived in the present investigation. There is, however, a tendency for the present values at shallow depths to lie below both the empirical relation and the early measurements. This discrepancy may be due to the different types of detectors employed such as those in which only coincidences are recorded between two layers of GM trays or plastic scintillators and those incor-

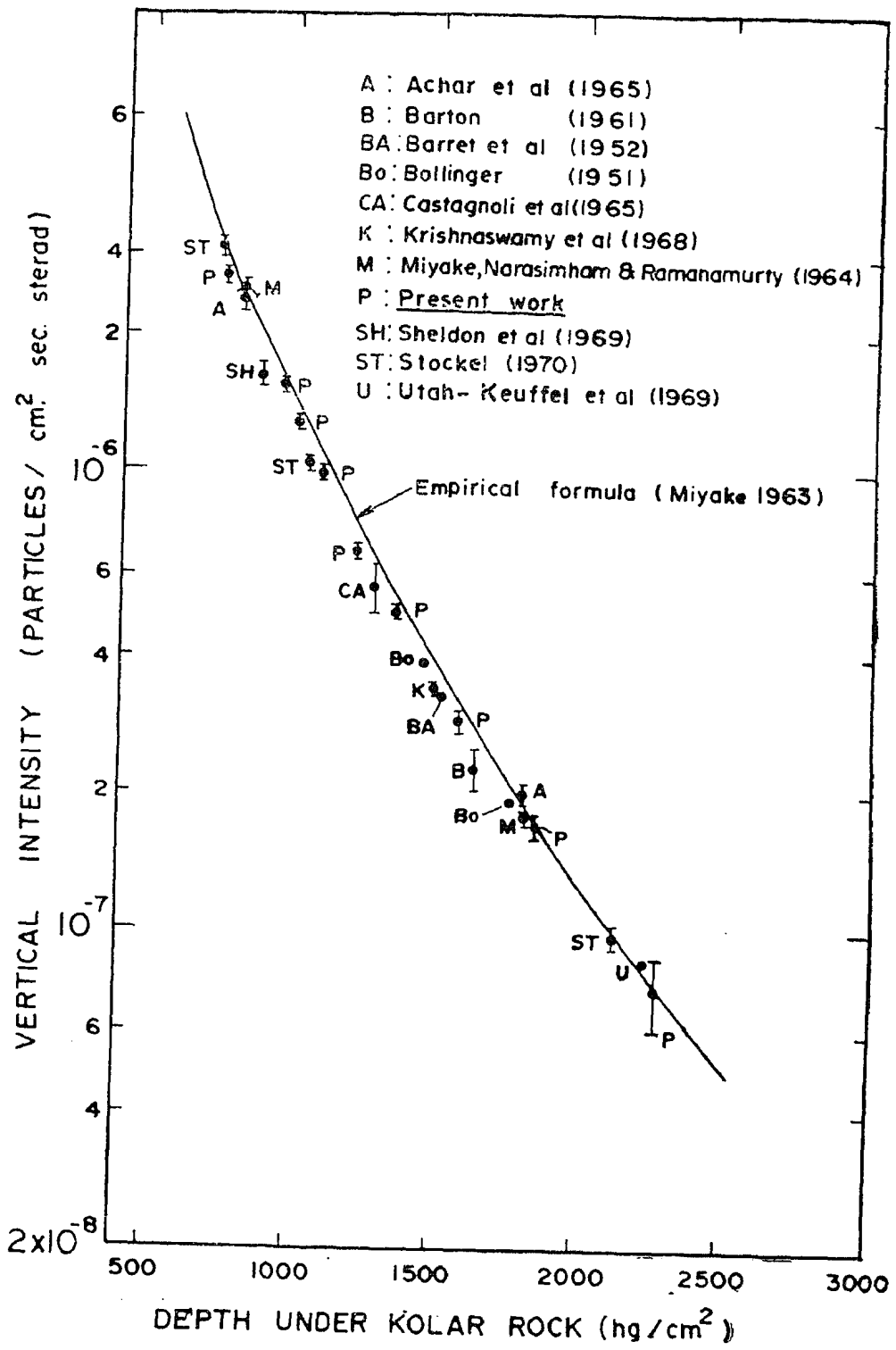

Figure 3. Vertical intensity *vs* depth relation under Kolar rock.

porating visual detectors (such as the present experiment). In the present experiment, we have recorded events (a few per cent of the cases), in which a muon enters the detector from outside, without traversing the scintillator, and the trigger is generated presumably by the soft component produced in the rock. Since the spacial angles of the track could be measured accurately, it was possible to identify such events unambiguously. Such a clear-cut classification will not be possible in detectors lacking detailed information concerning the tracks.

The excellent agreement between the vertical intensities measured directly, and those inferred from the angular distribution up to $\theta = 75°$ (*see* figure 3) demon-

strates clearly that atmospheric muons are produced wholly through the decay of pions and kaons up to energies of the order of 1000 GeV.

4.3. *K/π ratio*

Since the present data cover the energy range of muons sensitive to a variation in K/π ratio at production, it is, in principle, possible to estimate this ratio from the angular dependence of muons of a particular energy. Under the same terrain (*i.e.*, Kolar Gold Fields) and with the same detector, a measurement was made by us earlier (Krishnaswamy *et al* 1968) on the intensity of muons at 1500 hg/cm^2. This can be compared with the intensity at about $\theta = 60°$ from the present observations at 754 hg/cm^2 to obtain the K/π ratio corresponding to muons of energy ~ 500 GeV. An estimate can also be made of this ratio from the data available at all other angles; but for this the vertical intensities at the corresponding slant depths are not available as direct observations.

In figure 4, we plot the ratio, $I(\theta)/I_v$, namely the intensity observed in this experiment at an angle θ at the depth h, divided by the vertical intensity for the same amount of overburden, *i.e.*, $h \sec \theta$. For the vertical intensities we use the empirical relation (2) as well as the direct observation with the same detector at the depth of 1500 hg/cm^2. The expected values of $I(\theta)/I_v$, shown as a smooth

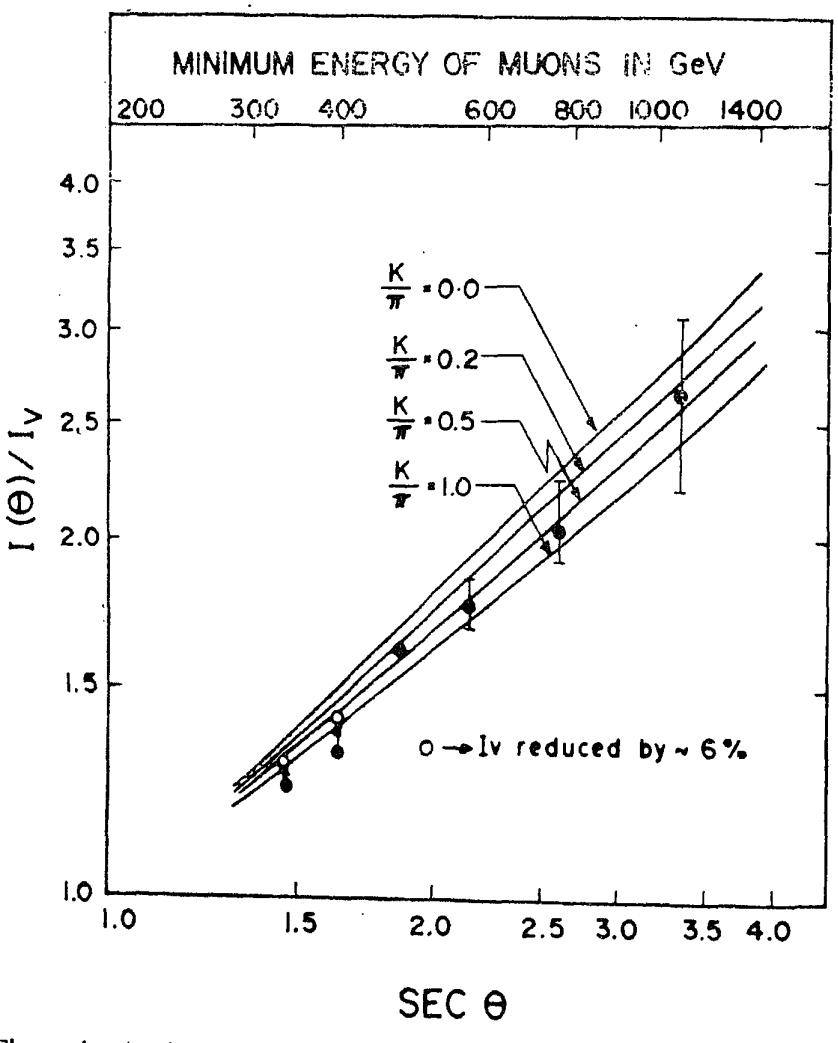

Figure 4. A plot of enhancement factors, $I(\theta)/I_v$ as a function of sec θ for different K/π ratios at production.

curve in this figure, are calculated for $K/\pi = 0$, $0{\cdot}2$, $0{\cdot}5$ and $1{\cdot}0$ using the method described in the previous section. We refer to the K/π ratio as the ratio of all kaons to all pions produced in nuclear collisions. The comparison clearly shows that the present measurements are consistent with a value of $K/\pi = 0{\cdot}3 \pm 0{\cdot}2$ at muon energies around 500 GeV. The statistical errors on the observations at very large angles do not allow a definite estimation to be made at higher muon energies; they are, however, consistent with the value obtained at 500 GeV.

The ratio of E_N, the nucleon energy, to E_μ, the muon energy, in the present observation is estimated as 8–10 assuming the scaling law to be valid in nuclear collisions over the TeV range of energies. Thus the K/π ratio determined here, for events with $\theta \sim 60°$, corresponds to nuclear collisions around 5 TeV, *i.e.*, energies considerably higher than those at the ISR (CERN). It is to be noted that within the statistical precision of the present data, the K/π ratio at these higher energies is consistent with that ($\sim 0{\cdot}15$) measured at ISR (CERN), which is the best available value in the TeV energy region.

In the past K/π ratio was estimated from cosmic ray observations such as the energy spectrum of muons at sea level as a function of zenith angle using magnet spectrographs. In general, the statistical accuracy of such data at high energies were rather poor and the K/π ratios determined from them have uncertainties of the order of 50%. The present observations are, however, consistent with them within the limited accuracies available.

It may be pointed out that some of the observed ratios for $\theta < 55°$ lie below the expected curves. This is easily understood as due to the fact that the vertical intensities *assumed* for the corresponding slant ranges are somewhat higher than those inferred from the present observations. If this correction is made, the agreement between the expected and the observed values in figure 4 will be excellent. This is demonstrated by correcting the vertical intensities by $\sim 6\%$ and plotting them in the same figure at two points in the angular region 30°–45°.

5. Parallel muons and rock showers

In this experiment, in addition to the single muons discussed so far, we have also observed events of the following types: (*a*) parallel-muon events in which there are at least two penetrating tracks parallel to each other within the angular resolution of the detector; and (*b*) rock showers produced as a result of the nuclear interaction of muons in the overlying rock.

5.1. *Parallel-muon events*

These events are considered as being due to muons, since their point of origin, within the uncertainties in the angle measurement, lies very deep inside the rock. Typically, for two vertically incident muons separated by about 1 m at the level of observation, their meeting point is > 10 m inside the rock, and therefore consistent with the assumption that their origin is in the upper layers oft he atmosphere. However, among the 2-track events with small separations of the order of 10 cm, there will be some events produced locally (by nuclear interaction of muons giving rise to a pion, for example), and which cannot be distinguished from parallel-muon events in view of the uncertainty in angle measurements ($\pm 1{\cdot}5°$). in the near

vertical directions. From the analysis of the rock shower events, discussed in section 5.2, this contamination is estimated to be small.

As mentioned in section 2, the triggering is provided by only 1 m^2 of the total scintillator area of 4 m^2. During the sensitive time of $8 \cdot 55 \times 10^5$ sec, the number of events recorded with 2, 3, 4 and 5 parallel muons are 93, 14, 3 and 1 respectively. These numbers have been corrected to correspond to the trigger by a 4 m^2 detector by assuming a uniform distribution of tracks in the 4 m^2 area. The correction factor is given by $1/[1-(3/4)^n]$ where n is the number of parallel tracks per event. These corrected numbers are plotted in figure 5 along with the number of single muons. The ratio of the number of parallel-muon events to single muons for 4 m^2 area of triggering is estimated from the present observations as $2 \cdot 2 \times 10^{-3}$.

The zenith angle distribution of parallel-muon events is shown in figure 6. Also shown here is the distribution of single muons with a suitable reduction in

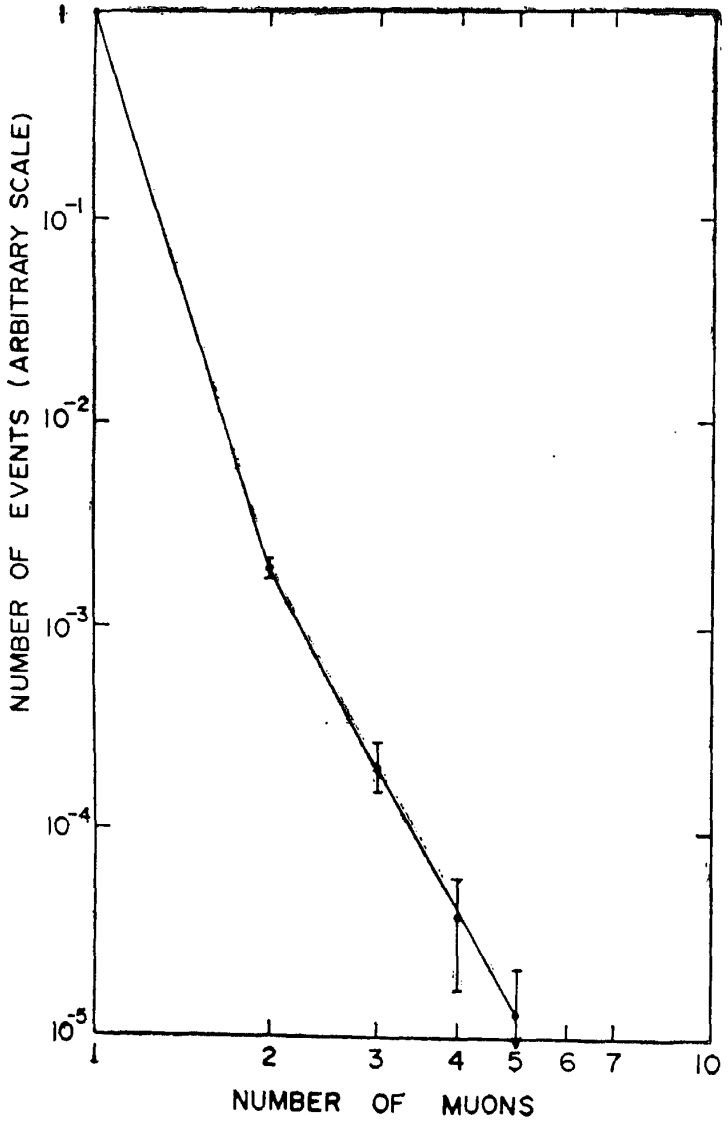

Figure 5. Multiplicity distribution of muon events observed at the depth of 754 hg/cm^2.

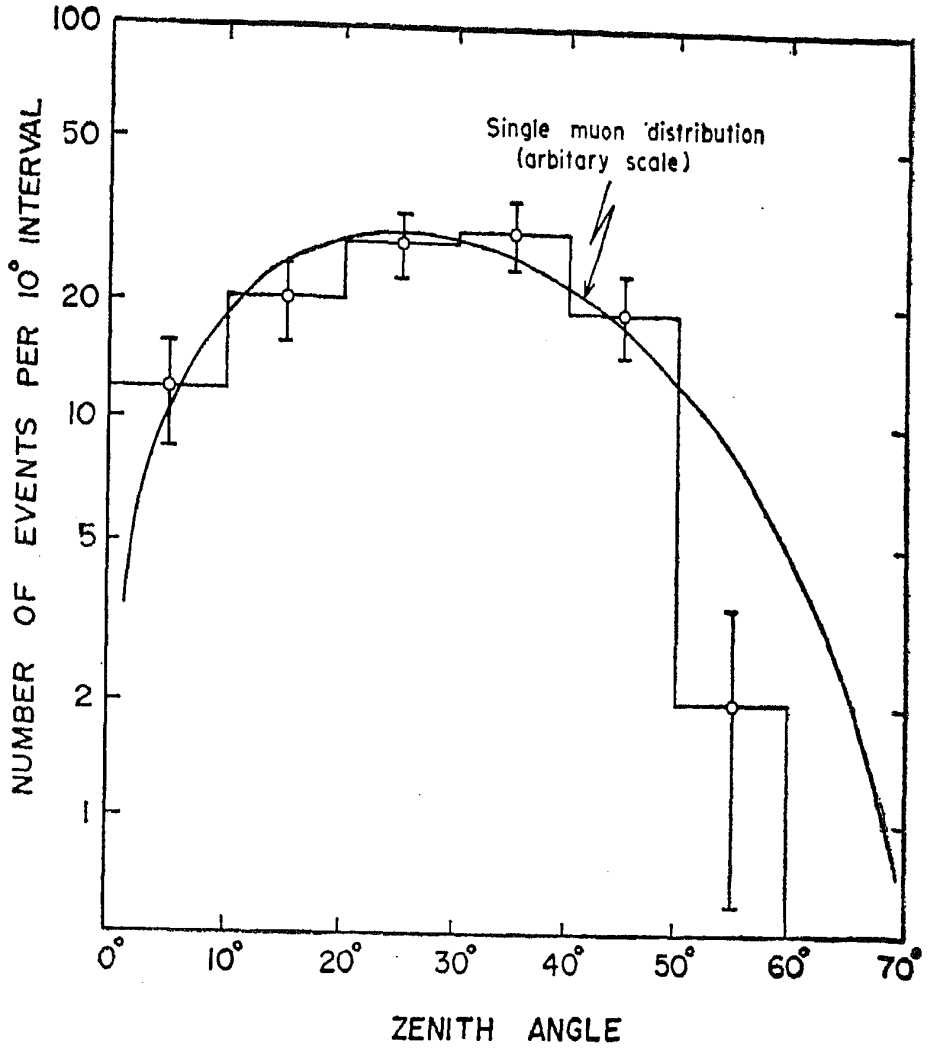

Figure 6. Angular distribution of parallel-muons; for comparison, the angular distribution of single muons is shown with an appropriately reduced scale.

scale. No correction has been made for the variation in the detection efficiency for multiple muons as a function of zenith angle. This effect is estimated to be small compared to the statistical accuracy of the data in the region 0°–40°, where most of the events are recorded. It is clear from the figure that the two distributions are of similar shape.

5.2. *Decoherence distribution*

We consider here two sets of data: (*a*) from the main telescope (figure 1) in which parallel muons are recorded up to a mutual separation of 2 m; (*b*) in association with a second telescope set at distances of 4·8 m and 10 m.

(*a*) *Decoherence in* 0–2 *m*

The events recorded in the area of 4 m^2 of the main telescope are considered for this analysis. As pointed out in the earlier sections, the trigger is provided only by 1 m^2 of the area at any time, so that at least one muon is within the 1 m^2 covered by the triggering detector and the other muons could be seen over the entire area. We normalise these data to correspond to a 4 m^2 trigger assuming a uniform distribution in this area. The number of events thus obtained for

each 25 cm interval is shown in figure 7. This is further corrected for efficiency of detection as a function of separation in a manner similar to that described by us earlier (Krishnaswamy *et al* 1969) and an effective decoherence distribution is obtained. This distribution is uniform within the statistical accuracy of the observations up to a separation of 2 m, consistent with the normal expectation that the multiple scattering of muons in passing through 754 hg/cm^2 of rock would smear out any non-uniformity of the original distribution within a meter.

(*b*) *Decoherence in* 0–10 *m*

The main telescope was operated for a part of the time in association with another telescope of area 1 m^2. The second telescope was made up of two plastic scintillators each of area 1 m^2 arranged one above the other and separated by a lead absorber of thickness 2·5 cm. Each scintillator was viewed by two photomultipliers of the type Dumont 6364. A 4-fold coincidence between the pulses from these photomultipliers indicated the passage of a muon through the telescope. This was, in turn, set in coincidence with a similar pulse from the main detector. For an event to be considered as due to multiple muons, there should be at least one muon passing through the triggering area of the main telescope where the track position and angle can be measured accurately. We estimate the chance coincidence due to noise in the second telescope to be negligible. Furthermore, based on the lateral extent and the frequency of the electro-

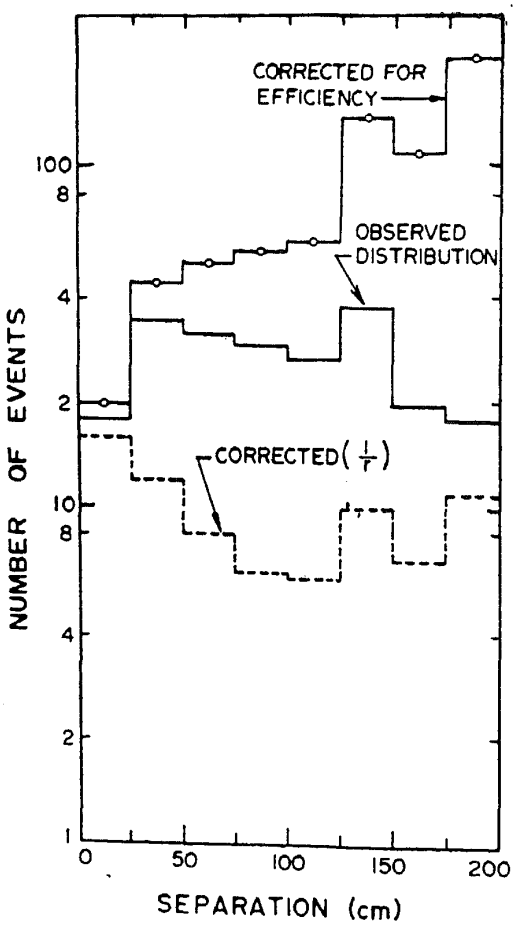

Figure 7. Decoherence distribution of parallel-muons in 0–2 m separation.

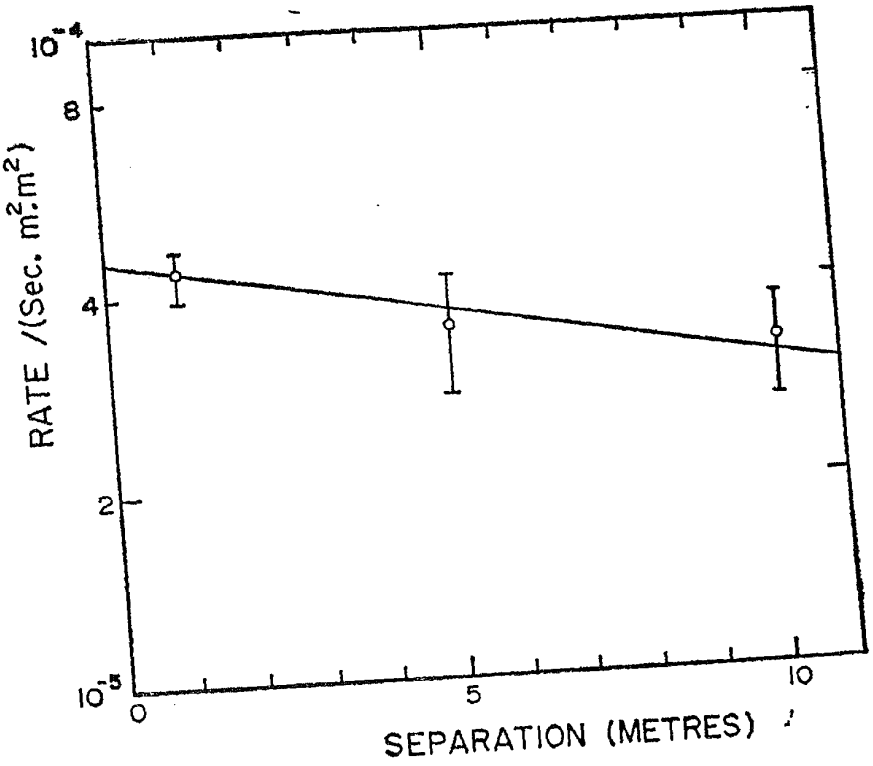

Figure 8. Decoherence distribution of parallel muons in 0–10 m separation.

magnetic showers seen in the main detector, we estimate that their contribution to the number of events recorded at separations of 5 m and 10 m is very small.

The telescopes were operated for $5{\cdot}99 \times 10^5$ seconds and $8{\cdot}67 \times 10^5$ seconds respectively at two separations of 4·8 m and 10 m (measured from centre to centre); the number of coincidences at these two separations were 21 and 28. The data presented in the earlier section for the main telescope have also been evaluated for 1 m separation between two detectors each 1 m² area, and from this we estimate the number of multiple muons to be 37·4 during a period of observation of $8{\cdot}55 \times 10^5$ sec. The resultant decoherence distribution is shown in figure 8 at average separations of 1 m, 4·8 m and 10 m. If we assume that the decoherence distribution can be expressed* as Ae^{-r/r_0}, the parameter 'r_0' can be closely related to the average transverse momentum, $\langle p_T \rangle$, of the parents of muons. The solid line in figure 8 is the best fit for such an exponential distribution with $A = (4{\cdot}5 \pm 0{\cdot}15) \times 10^{-5}$ (sec. m² . m²)$^{-1}$ and $r_0 = 28 \pm 5$ m. From this, we conclude that $\langle p_T \rangle$ of parents of muons with energy $\sim$250 GeV is $0{\cdot}3 \pm 0{\cdot}1$ GeV/c, in good agreement with ISR (CERN) measurements at comparable energies ($\sim$2 TeV) of primary interactions.

5.3. *Rock showers*

These events originate in the roof of the tunnel which is about 1·5 meters above the detector; the origins are distributed within a few meters inside the rock. A total

* Physically such a distribution can be visualized, if one considers the lateral spread of muons at the level of observation arising from the p_t distribution of pions and kaons producep at a variety of depths in the upper layers of atmosphere; the decoherence distribution, can then be approximated by an exponential form in the region of separations appropriate for our observations.

of 34 events were recorded with 1 m^2 triggering during the live time of $8{\cdot}55 \times 10^5$ sec. In order to normalise this number to the 4 m^2 area, correction factors were evaluated from the observed distribution of events in 1 m^2, 2 m^2, 3 m^2 and 4 m^2 area (with 1 m^2 triggering). The total number of rock showers, thus estimated, is 75 for a period of observation of $8{\cdot}55 \times 10^5$ sec for 4 m^2 area. This gives a ratio of the number of rock showers to single muons as $6{\cdot}82 \times 10^{-4}$. Following Barrett *et al* (1952), a comparison of this ratio with R_s/λ, where R_s is the range in rock of secondaries of muon interaction (assumed as 300 g/cm^2), and λ is the mean free path of muons to produce rock showers, gives a cross section for the nuclear interaction of muons as $3{\cdot}8 \times 10^{-30}$ cm^2/nucleon. In view of the uncertainties in the ranges of the showers in rock and also in the efficiency for the detection of such showers, the cross section is accurate only to $\sim 50\%$. The average energy of muons at this depth (754 hg/cm^2) is ~ 105 GeV. Assuming W–W approximation, the average nuclear cross section $\sigma_{\gamma n}$ for photons of energy $\gtrsim$ a few GeV is estimated from the present observation as $\sim 1{\cdot}5 \times 10^{-28}$ cm^2/nucleon.

In this paper, we have presented a simple analysis of the data on multiple muons and rock showers observed at this depth mainly from the experimental point of view. In a future publication, we shall combine them with the results from 1500, 3375 and 6030 hg/cm^2 and attempt to derive the characteristics of [illegible] and interaction particularly in terms of energy dependence in [illegible] region.

horities and staff of the Bharat Gold Mines Limited n which has made it possible to carry out the present r and H D Salvekar have provided able assistance our thanks are due to them. We are grateful to the ıne Promotion of Science and the Toray Scientific Fund t for the experiment.

References

Achar C V, Narasimham V S, Ramanamurthy P V, Creed D R, Pattison J B M and Wolfendale A W 1965 *Proc. Phys. Soc.* (London) **86** 1305.

Barrett P H, Bollinger L M, Cocconi G, Eisenberg Y and Greisen K 1952 *Rev. Mod. Phys.* **24** 133

Barton J C 1961 *Phil. Mag.* **6** 1271

Bollinger L M 1951 *Ph.D. Thesis*, Cornell University (unpublished)

Castagnoli C, De Marco A, Longhetto A and Penengo P 1965 *Nuovo Cim.* **35** 969

Keuffel J W, Osborne J L, Bolingbroke G L, Mason G W, Larson M O, Lowe G H, Parker J H, Stenerson R O and Bergeson H E 1969 *Acta Physica Hungarica* (Suppl. to Vol. 29) **4** 183

Krishnaswamy M R, Menon M G K, Narasimham V S, Kawakami S, Kino S and Miyake S 1968 *Phys. Lett.* **27B** 535

Krishnaswamy M R, Menon M G K, Narasimham V S, Kawakami S, Miyake S and Mizohata A 1969 *Acta Physica Hungarica* (Suppl. to Vol. 29) **4** 221

Maeda K 1964 *J. Geo. Res.* **69** 1725

Miyake S, 1963 *J. Phys. Soc.* (Japan), **18** 1093

Miyake S, Narasimham V S and Ramanamurthy P V 1964 *Nuovo Cim.* **32** 1505

Sheldon W R, Cantrell G, Bayer-Bachi R and St. Marc A 1964 *Acta Physica Hungarica* (Suppl. to Vol. 29) **4** 209

Stockel C J 1969 *J. Phys.* **2** 639